Edinburgh, Scotland

EURONOISE 2009

October 26-28

A 3D parabolic equation code for street canyon propagation

Bertrand Lihoreau[a]
Olivier Richoux
LAUM, CNRS, Université du Maine, avenue Olivier Messiaen, 72085 LE MANS, France.

ABSTRACT

The aim of this work is to study sound propagation in a U-shaped street canyon with reflecting building façades. A 3D parabolic equation is developed which takes into account meteorological conditions. We use the approximation of effective sound speed to consider temperature gradients and the convection effect of the wind. The source is initialized by a gaussian starter in the frequency domain and the propagation operator is simplified using a Padé approximation. The initial- and boundary-value problem is numerically solved using an alternating direction method. Numerical results show the modal behaviour of the sound field. Comparisons between experimental and numerical results are also presented.

1. INTRODUCTION

In urban areas, noise is one of the most important annoyance for citizens. Thus noise prediction is of major interest nowdays. Sound propagation calculations in urban areas focus mainly on sound propagation along streets. Applications of ray-tracing techniques (and improved variants thereof)[1] are numerous and lead to mainly commercial software[2]. The understanding of the importance of diffuse reflection on building façades led to the development of models based on the principle of radiosity[3] and models based on the linear transport equation and diffusion equation[4]. These methods are efficient for high frequency but fail in predicting wave effects as interference and diffraction. In the other hand, there are methods based on the wave equation such as *Finite Element Method* or *Boundary Element Method*. Recently, alternative models have been proposed to overcome numerical cost: the *Equivalent Source Method*[5] and the *Finite-Difference Time-Domain model*[6] which have been applied to an urban street canyon. The aim of this paper is to apply parabolic equation (PE) method[7] to study the wave propagation along streets. PE methods have been successfully used for outdoor sound propagation[8]. This method is able to take into account the mixed influence of ground characteristics (topography, obstacles, impedance, etc.) and atmospheric conditions (refraction and turbulence).

The paper is organized as follows. The next section describes the theoretical background. In section 3, numerical considerations are given. In section 4, the set-up of the scale model, the materials used and the way the obtained data have been analyzed. In section 5, numerical and experimental results are discussed and compared.

2. THEORETICAL BACKGROUND

We begin from the three-dimensional (3-D) Helmholtz equation in a homogeneous space for the acoustic pressure p, written in cartesian coordinates where x is the main direction of propagation (Fig 1) :

$$\frac{\partial^2 p}{\partial x^2} + \frac{\partial^2 p}{\partial y^2} + \frac{\partial^2 p}{\partial z^2} + k_0^2(1+\epsilon)p = 0. \tag{1}$$

[a]Email address. bertrand.lihoreau@univ-lemans.fr

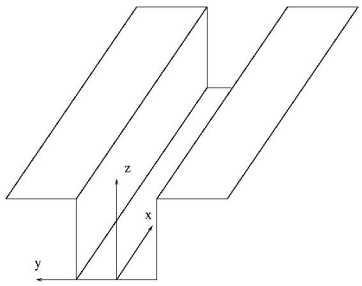

Figure 1: Domain

The complex pressure is $pe^{-i\omega t}$, where ω is the acoustic frequency. In Eq.(1), $k_0 = \omega/c_0$,$\epsilon = (c_0/c(x,z))^2 - 1$ is the variation of the standard refraction index. $c(x,z)$ is the sound speed and c_0 is a reference sound speed. Eq.(1) can be splitted into 2 equations for the outgoing wave (+) and the incoming wave (-). The equation for the outgoing wave is :

$$[\frac{\partial}{\partial x} - ik_0 Q]p^+ = 0, \tag{2}$$

where Q is the operator defined by

$$Q^2 = 1 + \epsilon + \frac{1}{k_0^2}(\frac{\partial^2}{\partial y^2} + \frac{\partial^2}{\partial z^2}). \tag{3}$$

If there is no coupling between outgoing and incoming waves, Eq.(2) represents an exact equation of the evolution of the acoustic pressure. It is more convenient to work with a scaled variable $\phi = p^+ e^{-ik_0 x}$ which leads to the one-way equation to solve :

$$\left(\frac{\partial}{\partial x} - ik_0(Q-1)\right)\phi = 0. \tag{4}$$

The solution of Eq. (4) is :

$$\phi(x+dx,z) = e^{ik_0(Q-1)dx}\phi(x,z). \tag{5}$$

The key point is to approxim the square root operator :

$$Q = \sqrt{1+\mathcal{L}_y+\mathcal{L}_z}, \tag{6}$$

with $\mathcal{L}_y = \frac{1}{k_0}\frac{\partial^2}{\partial y^2}$ and $\mathcal{L}_z = \epsilon + \frac{1}{k_0}\frac{\partial^2}{\partial z^2}$. It can be approximated using a higher order Padé approximation:

$$\sqrt{1+\mathcal{L}_y+\mathcal{L}_z} = 1 + \sum_{k=1}^{n_p}\frac{a_{k,n_p}\mathcal{L}_y}{1+b_{k,n_p}\mathcal{L}_y} + \sum_{k=1}^{m_p}\frac{a_{k,m_p}\mathcal{L}_z}{1+b_{k,m_p}\mathcal{L}_z}, \tag{7}$$

where n_p and m_p are the number of terms and a_{k,n_p}, b_{k,n_p} are real coefficients given in Ref. [9]. For 2D problems ($\mathcal{L}_y = 0$), the Padé series expansion allows a very wide angle propagation along z, the angular limitation depending on parameter n_p. However, this Padé approximation is not able to correctly describe the exponential decay of the physical evanescent modes. This is due to the fact that for evanescent modes, the pseudo-operator Q is complex whereas the Padé approximation remains real. Different authors introduced complex Padé expansion to overcome this problem[10]. In open space situation, evanescent modes are decreased by numerical absorbing layers (see in the following). In Eq. (7), we neglected terms in $\mathcal{O}(\mathcal{L}_y^{2n_p+1}, \mathcal{L}_z^{2m_p+1}, \mathcal{L}_y\mathcal{L}_z)$. Due to the term in $\mathcal{O}(\mathcal{L}_y\mathcal{L}_z)$, Eq. (5) does not, strictly speaking, have a wide-angle capability [11]. Thus, it seems coherent to make a Padé series expansion of order 1 with $a = 1/2$ and $b = 1/4$. In this case, Eq. 4 leads to:

$$\left(\frac{\partial}{\partial x} - ik_0(\frac{a\mathcal{L}_y}{1+b\mathcal{L}_y} + \frac{a\mathcal{L}_z}{1+b\mathcal{L}_z})\right)\phi = 0. \tag{8}$$

3. NUMERICAL RESOLUTION

The previous initial- and boundary- value problem is numerically solved using an alternating direction method [12], which requires numerical solutions for each of the following:

$$\frac{\partial \phi}{\partial x} = ik_0 \frac{a\mathcal{L}_z}{1 + b\mathcal{L}_z}\phi, \tag{9}$$

$$\frac{\partial \phi}{\partial x} = ik_0 \frac{a\mathcal{L}_y}{1 + b\mathcal{L}_y}\phi. \tag{10}$$

The alternating direction method allows us to compute only 2D problems (xz- planes for Eq. (9) and xy- planes for Eq. (10)). These equations are solved using a Crank-Nicholson integration in range and a finite difference method in depth and width.

We use a gaussian as a starting field ($x = 0$) :

$$\phi(0, y, z) = e^{-\frac{(y-y_s)^2+(z-z_s)^2}{w^2}} \tag{11}$$

where y_s and z_s are the position of the source and w is a parameter controlling the width of the gaussian. The radiation of the sound at infinity determines the upper bondary condition. As the PE method is solved on a finite height grid, a simulation of the radiation is required. For that purpose, we introduced a perfectly matched layer (PML)[13] above the street (Fig. 1). Note that the CPU time remains less than 1 minutes for all simulations with a spacial sampling step of about $\lambda/20$.

4. EXPERIMENTAL SET-UP

Measurements are performed in a 1/25 scale model of 6.75 m height and 5 m width (Fig. 2). The scale model is put in a semi-anechoic room. Building facades are simulated by wood cubes. For this work, the cubes distribution is plane. An anechoic terminaison made of foam dihedron is put at the end of the street to simulate a semi infinite street. A loudspeaker embedded in a rigid box is used as an acoustic source. It is fixed on a rigid wall which closes the other end of the street. The wall contains a small aperture for the sound to come into the street.
The acoustic pressure is measured by means of two 1/4 in. microphones (B& K) associated with their preamlifiers (B& K) and conditionning amplifiers (B& K). The first microphone measures the acoustic pressure in the loudspeaker box and acts as a control microphone. The second microphone has its position driven by a 3D-robot which allow us to map the acoustic pressure in the street.

The loudspeaker provides a sinusoidal signal of frequency f.

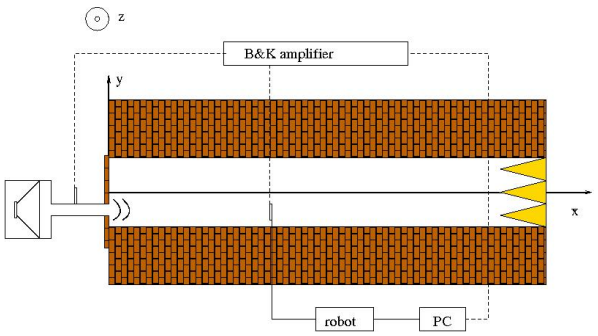

Figure 2: Experimental set-up in the $x - y$ plane.

5. RESULTS AND DISCUSSION

In this section, experimental results are presented. We study the pressure field in a horizontal plane at a height corresponding to the height of the source z_s. Figure 3 shows acoustic pressure along the street for $f = 2000\ Hz$ (80 Hz equivalent full scale) with a source locating at $y_s = 0.02\ m$ and $z_s = 0.07\ m$. The figure on the top corresponds to the PE code simulation whereas the figure on the bottom corresponds to experimental results. These maps show the modal behaviour of the acoustic field. The acoustic pressure globaly decreases along x due to losses by the open roof. Nevertheless, one can observe discrepancies at the begining of the street. This is due to the fact that the gaussian source we use for the numerical simulation is significatively different from the real source.

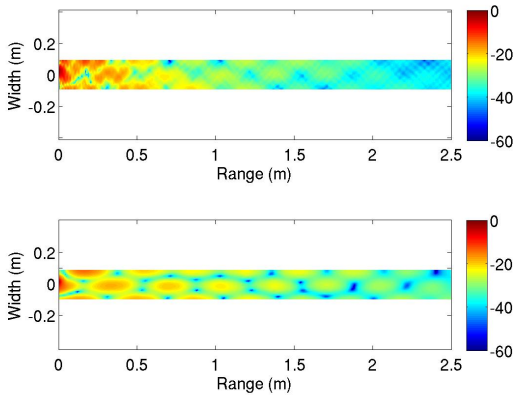

Figure 3: Numerical (top) and experimental (bottom) results at $z = z_s$ for $f = 2000\ Hz$. The source is located at $y_s = 0.02\ m$, $z_s = 0.07\ m$.

For a more quantitave comparison, we plot on Fig. 7 numerical (blue dash) and experimental (red) attenuation along the x-axis in front of the source. One can observe a very good agreement between experimental and numerical results. The positions of the maxima and the minima are very well predicted. Furthermore, the global attenuation is also well predicted. The PE model seems to be able simulate the acoustic energy which run away by the open roof.

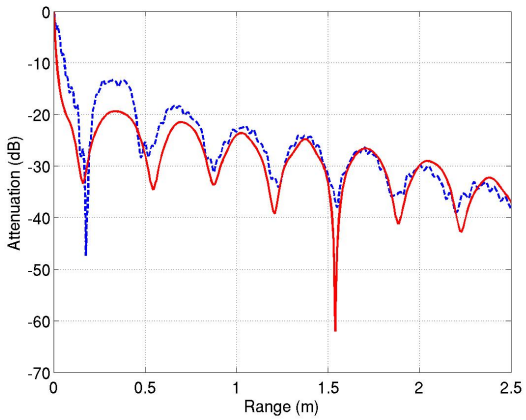

Figure 4: Comparison of experimental (red curve) and numerical (blue dash) results along the street in front of the source ($y_s = 0.02\ m$, $z_s = 0.07\ m$) for $f = 2000\ Hz$.

Fig. 5 and fig. 6 shows the same data than fig. 3 and fig. 4 except that the source is now located at $y_s = 0\ m$ and the frequency is $f = 2500\ Hz$ (100 Hz equivalent full scale). Numerical predictions are still very good but one can observe on Fig. 6 that numerical minimas are lower than experimental

ones. This can be due to the spatial sampling for the experiences which is 0.01 m and to the spatial integration of the pressure field over the microphone's diaphragm.

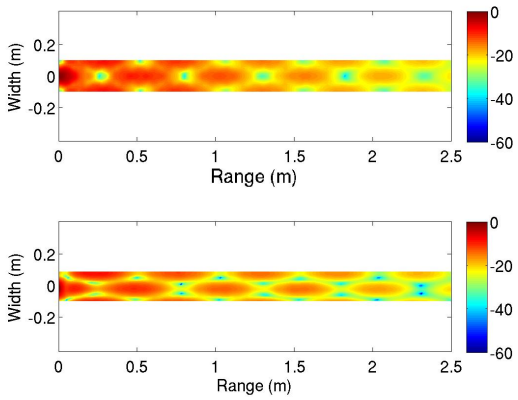

Figure 5: Numerical (top) and experimental (bottom) results at $z = z_s$ for $f = 2500\ Hz$. The source is located at $y_s = 0\ m$, $z_s = 0.07\ m$.

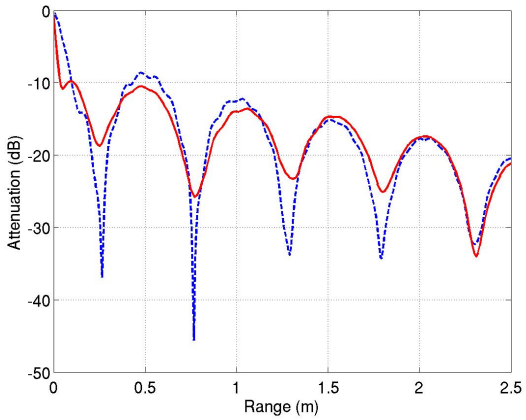

Figure 6: Comparison of experimental (red curve) and numerical (blue dash) results along the street in front of the source ($y_s = 0\ m$, $z_s = 0.07\ m$) for $f = 2500\ Hz$.

At last, we present maps to study the micrometeorological effets. To simplify the problem, the mean vertical sound speed profiles are set constant along the distance and are logarithmically shaped as previously presented by Gilbert and White[14]:

$$c(z) = c_0 + a_{eff} ln(z/z_0), \tag{12}$$

where z_0 is the roughness parameter and a_{eff} an effective refraction parameter[8]. Figure 7 shows maps representing the sound pressure level in a horizontal plane in front of the source with the same parameters than Fig. 5. The figure on the top corresponds to an upward refraction ($a = -2\ m/s$) while figure on the bottom correponds to a downward refraction ($a = 2\ m/s$). These values for the effective refraction parameter are usual in outdoor situation. We can see the strong effect of refraction on the acoustic attenuation along the street. This effect are especially dramatic for upward refraction and can lead to a dicrease of order 20 dB since a distance of 1 m from the source (25 m in full scale). Finally, we can note that downward refraction has a weak effect on sound level but tends to break the modal behaviour of the acoustic field.

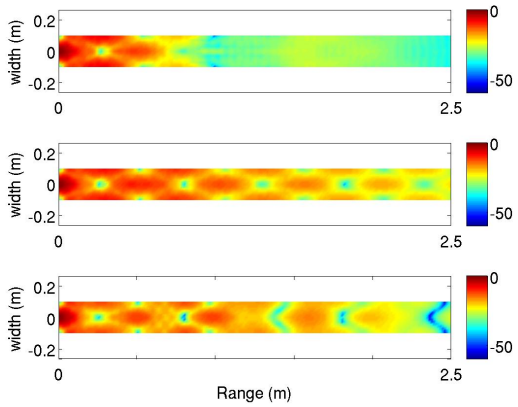

Figure 7: Meteorological effects on sound pressure level. The effective refraction parameter is $a_{eff} = -2\ m/s$ (top), $a_{eff} = 0\ m/s$ (middle), $a_{eff} = 2\ m/s$ (bottom). The parameters are the same than those used for Fig. 5

6. CONCLUSION

In this paper, it has been shown that three-dimensional parabolic equation model can provide very effective and accurate simulation of the acoustic propagation in a street canyon. The experimental results are obtained with a scale model describing a semi-infinite 6.75 m height and 5 m width street. Three phenomenon have been pointed out. The first one is losses due to the radiations by the street roof. Our model is able to correctly describe the leakage of the wave. The second phenomenon is the modal behaviour of the acoustic field. This behaviour can't be simulated with a ray-type model. At last we show that atmospheric refraction could have a dramatic effect on sound pressure level and on the field's structure.

This work opens the field for further investigations, notably the more precise description of sound speed profiles in urban environment. Outdoor controlled experiments will be realized in order to validate the code for such complex configurations.

ACKNOWLEDGMENTS

This work was supported by the Regional council of the Pays de La Loire.

REFERENCES

1. K. Heutschi, A simple method to evaluate the increase of traffic noise emission level due to buildings for a long straight street, *Appl. Acoust.* **44**, pp. 259-274 (1995).
2. ISO 9613-2. Attenuation of sound during propagation outdoors â Part 2: general methods of calculation. Obtainable from the International Organization for Standardization. Available from: http://www.iso.org.
3. J. Kang, Numerical modelling of the sound fields in urban streets with diffusely reflecting boundaries, *J. Sound Vib.* **258**(5), pp. 793-813 (2002).
4. J. Picaut, L. Simon, and J. Hardy, Sound field modelling in a street with a diffusion equation, *J. Acoust. Soc. Am.* **106**, pp. 2638-2645 (1999).
5. M. Ögren and J. Forssén, Modelling a city canyon problem in a turbulent atmosphere using an equivalent source approach, *Appl. Acoust.* **65**(6), pp. 629-642 (2004).
6. D. Heimann, Three-dimensional linearised Euler model simulations of sound propagation in idealised urban situations with wind effects, *Appl. Acoust.* **68**(2), pp. 217-237 (2006).

7. F. D. Tappert, Wave propagation in underwater acoustic, chap. 5,*Springer-Verlag*, pp. 224-285 (1977).
8. B. Lihoreau, B. Gauvreau, M. Bérengier, Ph. Blanc-Benon and I. Calmet, Outdoor sound propagation modeling in realistic environments: Application of coupled parabolic and atmospheric models *J. Acoust. Soc. Am.* **120**(1), pp. 110-119 (2006).
9. A. Bamberger, B. Engquist, L. Halpern and P. Joly, Higher order paraxial wave equation approximations in heterogeneous media, *SIAM J. Appl. Math.* **5**, pp. 129-154 (1988).
10. Y.Y. Lu, A complex coefficient rational approximation of root 1+x, *Appl. Num. Math.* **27**(2), pp. 141-154 (1998).
11. F. Collino and P. Joly, Splitting of operators, alternate directions, and paraxial approximations for three-dimensional wave equation, *SIAM J. Sci. Comput.* **16**(5), pp. 1019-1048 (1995).
12. M.D. Collins and S.A. Ching-Bing, A three dimensional parabolic equation model that includes the effect of rouh boundaries, *J. Acoust. Soc. Am.* **81**, pp. 1104-1109 (1990).
13. D. Yevick and D. J. Thomson, Impedance-matched absorbers for finite difference parabolic equation algorithms, *J. Acoust. Soc. Am.* **107**(3), pp. 1226-1234 (2000).
14. K. E. Gilbert and M. J. White, Application of the parabolic equation to sound propagation in a refracting atmosphere, *J. Acoust. Soc. Am.* **85**, pp. 630-637 (1989).